NONAUTONOMOUS SPATIOTEMPORAL SOLITONS IN THE HARMONIC EXTERNAL POTENTIAL

Chao-Qing Dai[†]

School of Sciences, Zhejiang A&F University
Lin'an, Zhejiang 311300, P.R. China

Yun-Jie Xu

School of Engineering, Zhejiang A&F University
Lin'an, Zhejiang 311300, P.R. China

(Received November 21, 2011; revised version received January 9, 2012)

A series of analytical nonautonomous soliton solutions for the (3+1)-dimensional nonlinear Schrödinger equation with variable coefficients in the presence of gain (loss) and a harmonic potential are obtained. The explicit functions which describe the evolution of the amplitude, phase and velocity are also given. Soliton's phase and velocity are independent of the gain parameter, and only the amplitude is affected by the gain parameter. The dynamical behaviors for nonautonomous chirp-free and chirped solitons in a periodic distributed and dispersion decreasing systems are discussed. By modulating appropriate diffraction/dispersion parameters, we can trap the velocity of each soliton to control the interaction between soliton pairs. The real and imaginary parts of the spectral parameters control the separating or interacting behavior of chirp-free soliton pairs. However, the appearance of the chirp restrains the interaction between the chirped soliton pairs.

DOI:10.5506/APhysPolB.43.367
PACS numbers: 05.45.Yv, 42.81.Dp, 42.65.Tg

1. Introduction

So far, colored nonautonomous solitons in nonlinear and dispersive nonautonomous physical systems governed by the nonlinear Schrödinger equations (NLSEs) have attracted much attention in many different fields, such as nonlinear optics [1, 2] and Bose–Einstein condensations (BECs) [3, 4]. Nonautonomous solitons, which were introduced by Serkin *et al.* in 2007 [4],

[†] Corresponding author: dcq424@126.com

are corresponding to the classical solitons. It is well-known that for the classical solitons, time (or space coordinate in the case of spatial optical solitons) only plays the role of the independent variable and does not appear explicitly in the nonlinear evolution equations. Nonautonomous solitons in nonautonomous physical systems exist only under certain conditions (exact integrability conditions) and varying in time nonlinearity cannot be chosen independently; they generally move with varying amplitudes, speeds and spectra adapted both to the external potentials and to the dispersion and nonlinearity variations.

Recently, exactly controllable transmission of nonautonomous optical solitons was discussed in [5]. Nonautonomous soliton dispersion management was also studied in [6]. More recently, Serkin *et al.* [7] investigated the optical and matter-wave 3D nonautonomous soliton bullets. Cai *et al.* [8] discussed the formation and propagation of self-similar solitary wave family in Kerr nonlinear media with external Bessel lattice. These nonautonomous solitons are governed by the nonautonomous NLSEs or Gross–Pitaevskii equations (GPEs). Xu *et al.* and Zhong *et al.* [9] got two kinds of nonautonomous soliton solutions by the F-expansion method. Beitia *et al.* [10] and Xia *et al.* [11] obtained periodic localized solutions by reducing the (1+1)-dimensional and (2+1)-dimensional NLSEs with spatially modulated parameters into the stationary NLSEs, respectively. Furthermore, Zhao *et al.* [5] and Dai *et al.* [12] derived exact solutions by reducing the inhomogeneous NLSEs into the standard NLSEs.

Note that many authors [5,6,10] discussed nonautonomous solitons only in (1+1)-dimension, although the (3+1)-dimensional single soliton solutions have been obtained in [9]. Relatively less research work for higher-dimensional NLSEs with the external potential was carried out. Moreover, in practice, due to the nonlinearity, the interaction between solitons is inevitable. A natural and important issue is how to obtain the (3+1)-dimensional nonautonomous multi-soliton solutions. In this paper, we wish to obtain more abundant nonautonomous solitons than those in [9] by using the similarity transformation method. The paper is organized as follows. In Section 2, we describe and apply the similarity transformation method to the (3+1)-dimensional nonautonomous NLSE with a harmonic potential. In Section 3, we introduce exact nonautonomous soliton pair solutions and devote to analyzing shape-changing collisions exhibited by these soliton pair solutions when different systems are employed. In the final section, the outcomes are summarized.

2. The model and the similarity transformation method

We study the (3+1)-dimensional generalized NLSE with variable coefficients in the presence of gain (loss) γ and a harmonic potential Vr^2 in the form [9]

$$iu_t + \frac{\beta_1(t)}{2}\triangle_\perp u + \frac{\beta_2(t)}{2}u_z + \chi(t)|u|^2u + V(t)r^2u = i\gamma(t)u\,, \tag{1}$$

where $u(t,x,y,z)$ denotes the spatiotemporal field envelope, t is the evolutional time, $\triangle_\perp = \partial_x^2 + \partial_y^2$ is the transverse Laplacian, $r = \sqrt{x^2+y^2+z^2}$ is the position coordinate and $V(t)$ stands for the strength of the harmonic potential which is related to the strength of the electric field established in the medium. The functions $\beta_1(t)$, $\beta_2(t)$, $\chi(t)$ and $\gamma(t)$ represent the diffraction, dispersion, nonlinearity and gain or loss coefficients, respectively. In the context of BECs, equation (1) is also called the GPE which describes the evolution of matter waves. The NLSE (GPE) model is a ubiquitous and significant model that appears in numerous branches of physics, such as nonlinear optics, condensed matter physics, BECs, plasma physics and hydrodynamics.

Especially, when $\beta_1(t) = \beta_2(t)$, Eq. (1) is the nonlinear GPE in [13, 14], where single soliton solutions have been obtained by the F-expansion method. For $\beta_1(t) = 0$, Eq. (1) can be reduced to the (1+1)-dimensional GPE in [15], where single soliton solutions have also been derived by the F-expansion method. By exchanging t and z, it represents the (1+1)-dimensional NLSE with distributed nonlinear gain governing the propagation of the optical field in a single-mode optical fiber [16]. In particular, when $V(t) = 0$ and exchanging t and z, Eq. (1) can be reduced to the (3+1)-dimensional NLSE [12], (2+1)-dimensional NLSE [17] and (1+1)-dimensional NLSE [2] in nonlinear optics.

Our strategy is to reduce the nonautonomous NLSE (1) into the autonomous one by a similarity transformation. Then, by making the reverse transformation variables and functions, we obtain the exact nonautonomous soliton solutions for Eq. (1). Solutions of Eq. (1) can be obtained from known solutions of the autonomous NLSE (2) by exploiting a one-to-one correspondence. Since abundant and well-known solutions exist in the autonomous NLSE, we can also construct rich and important nonautonomous soliton solutions of Eq. (1).

To connect Eq. (1) with the autonomous NLSE

$$iU_T + \tfrac{1}{2}U_{XX} + \sigma|U|^2U = 0\,, \tag{2}$$

where $T = T(t)$, $X = X(t,x,y,z)$, we will use the similarity transformation used to appear in (1+1)D case [16, 18]

$$u(t,x,y,z) = A(t)e^{i\phi(t,x,y,z)}U(T,X)\,, \tag{3}$$

where $\sigma = 1$ and $\sigma = -1$ lead to bright and dark multisoliton solutions, respectively. Note that the reduced (1+1)-dimensional autonomous NLSE (2) is more general than the stationary NLSE or the elliptic equation for the F-expansion method in [5,6,10,13,14,15,17], where no exact nonautonomous multi-solitons were obtained.

Requiring U to satisfy Eq. (2) and u to be a solution of Eq. (1), we get the set of equations

$$A_t + \tfrac{1}{2}\beta_1 A \triangle_\perp \phi + \tfrac{1}{2}\beta_2 A\phi_{zz} - \gamma A \;=\; 0\,, \tag{4}$$

$$X_t + \beta_1 \nabla_\perp X \nabla_\perp \phi + \beta_2 X_z \phi_z \;=\; 0\,, \tag{5}$$

$$\phi_t + \tfrac{1}{2}\beta_1 \triangle_\perp \phi + \tfrac{1}{2}\beta_1 \phi_z^2 - Vr^2 \;=\; 0\,, \tag{6}$$

$$\beta_1 \triangle_\perp X + \beta_2 X_{zz} \;=\; 0\,, \tag{7}$$

$$\beta_1 |\nabla_\perp X|^2 + \beta_2 X_z^2 = T_t\,, \qquad A^2\chi = \sigma T_t\,. \tag{8}$$

By solving these equations self-consistently, we get a set of conditions on the coefficients and parameters necessary for Eq. (1) to have exact nonautonomous solutions. We consider the most generic case, that is, $\beta_1(z)$, $\beta_2(z)$ and $\gamma(z)$ are arbitrary. It is difficult to solve Eqs. (4)–(8), here we find some simplest particular solutions for the following two cases. However, these simplest particular solutions obtained here are more general than those in the corresponding literatures [9, 13].

3. Nonautonomous chirp-free and chirped soliton pairs

Firstly, we consider $V(t) = 0$, then from Eqs. (4)–(8), one can obtain the amplitude, phase, accumulated time and similarity variable as follows

$$A = A_0 \exp\left[\varGamma(t)\right], \qquad \phi = p(x+y+z) - \tfrac{1}{2}p\int_0^t [2\beta_1(\tau)+\beta_2(\tau)]dt + \phi_0\,, \tag{9}$$

$$T = \int_0^t \left[\left(k^2+l^2\right)\beta_1(\tau) + q^2\beta_2(\tau)\right] dt + T_0\,, \tag{10}$$

$$X = kx + ly + qz - p(k+l)\int_0^t \beta_1(\tau)dt - pq\int_0^t \beta_2(\tau)dt + \omega_0\,, \tag{11}$$

where the accumulated gain/loss $\mathit{\Gamma}(t)=\int_0^t \gamma(\tau)dt$, and k, l, q, p are all constants. The subscript 0 denotes the initial values of the corresponding parameters at time $t=0$.

Further, the necessary and sufficient condition for the existence of such chirp-free solutions is given by the following relationship between the parameters

$$\chi(t)=\frac{\sigma \exp[-2\mathit{\Gamma}(t)]}{A_0^2}\left[\left(k^2+l^2\right)\beta_1(t)+q^2\beta_2(t)\right], \tag{12}$$

from which we know that if parameters $\beta_1(t)$, $\beta_2(t)$ and $\gamma(t)$ in Eq. (1) are chosen to be free parameters, then $\chi(t)$ will be determined from Eq. (12).

In the following, we consider the chirped phase case. From Eqs. (4)–(8), one can obtain the amplitude, phase, accumulated time, similarity variable and dispersion/diffraction parameters as follows

$$A=A_0[C_p(t)+c_0]^{3/2}\exp\left[\mathit{\Gamma}(t)\right], \tag{13}$$

$$\phi=C_p(t)\left(x^2+y^2+z^2\right)+p\left[C_p(t)+c_0\right](x+y+z)+\tfrac{3}{4}p^2\left[C_p(t)+c_0\ln C_p(t)\right]+\phi_0, \tag{14}$$

$$T=-\tfrac{1}{2}\left(k^2+l^2+q^2\right)\left[C_p(t)+c_0\ln C_p(t)\right]+T_0, \tag{15}$$

$$X=C_p(t)(kx+ly+qz)-\tfrac{1}{2}p(k+l+q)\left[C_p(t)+c_0\ln C_p(t)\right]+\omega_0, \tag{16}$$

$$\beta_1(t)=\beta_2(t)=\beta(t)=-\frac{1}{2C_p(t)\left[C_p(t)+c_0\right]}\frac{dC_p}{dt}, \tag{17}$$

where the chirp function $C_p(t)$ is related to the diffraction/dispersion parameter $\beta(t)$, and constant c_0 is not equal to zero.

For the chirped solution, the nonlinearity coefficient $\chi(t)$ satisfies

$$\chi(t)=-\frac{\sigma\left(k^2+l^2+q^2\right)\exp[-2\mathit{\Gamma}(t)]}{2A_0^2C_p(t)[C_p(t)+c_0]^2}\frac{dC_p}{dt}, \tag{18}$$

and the strength of the harmonic potential $V(t)$ is determined from the following equation

$$V(t)=-2c_0C_p(t)\beta(t). \tag{19}$$

Employing the transformation (3) and Darboux transformation (DT) [19], one can obtain bright multi-solitons for Eq. (1)

$$u=A(t)e^{i\phi(t,x,y,z)}\left[u_0+2\sqrt{1/\sigma}\sum_{m=1}^{n}\frac{(\lambda_m+\lambda_m^*)\varphi_{1,m}(\lambda_m)\varphi_{2,m}^*(\lambda_m)}{A_m}\right], \tag{20}$$

with

$$\begin{aligned}\varphi_{j,m+1}(\lambda_{m+1}) &= (\lambda_{m+1}+\lambda_m^*)\varphi_{j,m}(\lambda_{m+1}) - \frac{B_m}{A_m}(\lambda_m+\lambda_m^*)\varphi_{j,m}(\lambda_m)\,,\\ A_m &= |\varphi_{1,m}(\lambda_m)|^2 + |\varphi_{2,m}(\lambda_m)|^2\,,\\ B_m &= \varphi_{1,m}(\lambda_{m+1})\varphi_{1,m}^*(\lambda_m) + \varphi_{2,m}(\lambda_{m+1})\varphi_{2,m}^*(\lambda_m)\,,\end{aligned} \tag{21}$$

where DT $\times\, m = 1,\ldots,n$, $j = 1,2$, complex spectral parameters $\lambda_m = \frac{1}{2}(\eta_m + i\xi_m)$, λ_m^* is the complex conjugate of λ_m. $T, X, A(t)$ and $\phi(t,x,y,z)$ satisfy Eqs. (9)–(11) for chirp-free soliton and Eqs. (13)–(16) for chirped soliton. $(\varphi_{1,1}(\lambda_1), \varphi_{2,1}(\lambda_1))^T$ is the eigenfunction corresponding to λ_1 for u_0 and $\varphi_{j,1} = \exp(\frac{\delta_j}{2} + i\frac{\kappa_j}{2})$, with

$$\delta_j = \eta_j X - \eta_j \xi_j T - \delta_{j0}\,, \qquad \kappa_j = \xi_j X - \tfrac{1}{2}\left(\eta_j^2 - \xi_j^2\right)T - \kappa_{j0}\,. \tag{22}$$

Inserting the zero seeding solution of Eq. (1) as $u_0 = 0$ into Eq. (20), one can obtain one-soliton solution for Eq. (1). Using that one soliton solution as the seed solution in Eq. (20), we can obtain two-solitons. Thus in recursion, one can generate up to n-solitons. Because bright one soliton has been obtained in [9], here we present bright two-soliton solutions in the explicit form

$$u = \sqrt{1/\sigma}\,A(t)e^{i\phi(t,x,y,z)}G_1/F_1\,, \tag{23}$$

where $G_1 = a_1\cosh\delta_2 e^{i\kappa_1} + a_2\cosh\delta_1 e^{i\kappa_2} + ia_3(\sinh\delta_2 e^{i\kappa_1} - \sinh\delta_1 e^{i}\kappa_2)$, $F_1 = b_1\cosh(\delta_1+\delta_2) + b_2\cosh(\delta_1-\delta_2) + b_3\cos(\kappa_2-\kappa_1)$, $a_j = \frac{\eta_j}{2}[\eta_j^2 - \eta_{3-j}^2 + (\xi_1-\xi_2)^2]$, $b_j = \frac{1}{4}\{[\eta_1 + (-1)^j\eta_2]^2 + (\xi_1-\xi_2)^2\}$, $a_3 = \eta_1\eta_2(\xi_1-\xi_2)$ and $b_3 = -\eta_1\eta_2$, $j = 1,2$. δ_j and κ_j are given by Eq. (22).

Moreover, we can also derive chirp-free and chirped dark (gray) multi-solitons for Eq. (1) by the DT. Here we pay our attention to the exact gray soliton pairs

$$u = \mu\sqrt{-1/\sigma}\,A(t)e^{i[\phi(t,x,y,z)+\psi(T,X)]}\left(1 + G_2/F_2\right)\,, \tag{24}$$

where $G_2 = 4\mu(\omega_1+\omega_2-2\mu) - 4i\frac{\lambda_1+\lambda_2}{\eta_1+\eta_2}\varrho$, $F_2 = 4\mu^2 + (\frac{\lambda_1+\lambda_2}{\eta_1+\eta_2})^2\varrho$, $\varrho = (\omega_1-\mu)(\omega_2-\mu)$, $\omega_j = (\xi_j - i\eta_j)[\xi_j + i\eta_j\tanh(\delta_j)]/\mu$, $\delta_j = \eta_j[X - X_{j0} + B(\Omega+\xi_j)T]$, $\psi(T,X) = -B(\mu^2 + \frac{\Omega^2}{2})T - \Omega X - \psi_0$, $\lambda_j = \xi_j + i\eta_j$ and $\mu = |\lambda_j|$, $j = 1,2$. $T, X, A(t)$ and $\phi(t,x,y,z)$ satisfy Eqs. (9)–(11) for chirp-free soliton and Eqs. (13)–(16) for chirped soliton.

4. The dynamic behaviors of nonautonomous chirp-free soliton pairs

Next, major attention will be paid to analyze the management of nonautonomous chirp-free solitons in some typical nonlinear media. The first one is the periodic distributed system [3, 4, 9, 16] when the periodic varying dispersion/diffraction parameters $\beta_1(z) = \beta_{10}\cos(\omega_1 z)$, $\beta_2(z) = \beta_{20}\cos(\omega_2 z)$ and a small constant gain/loss parameter $\gamma = \gamma_0$ are included. This management system leads to alternating regions of positive/negative values [*cf.* Fig. 1 (a)] of both $\beta_1(t)$, $\beta_2(t)$ and χ, which are required for an eventual stability of soliton solutions [17]. As shown in Fig. 1 (b), another example is the dispersion decreasing fiber (DDF) with the dispersion/diffraction and the nonlinearity parameter [9, 19] according to $\beta_1(z) = \beta_{10}\exp(\omega_1 z)$, $\beta_2(z) = \beta_{20}\exp(\omega_2 z)$ and a small constant gain/loss parameter $\gamma = \gamma_0$.

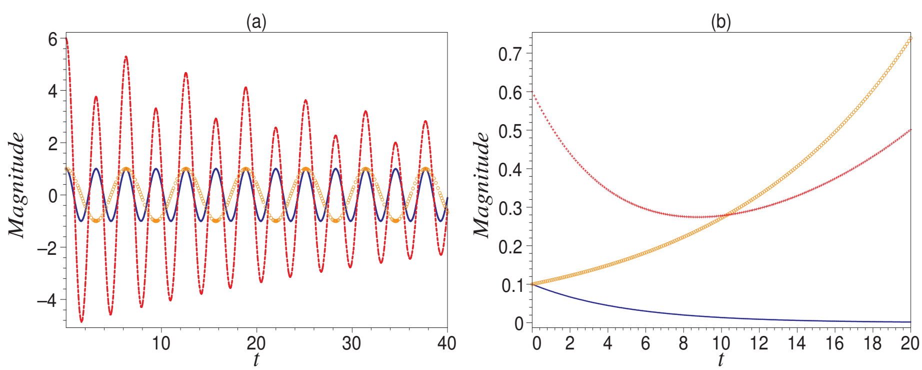

Fig. 1. (Color online) (a) and (b) depict respectively periodic and dispersion decreasing systems. The parameters are chosen as $A_0 = k = q = 1$, $l = 2, \sigma = 1$, $\gamma_0 = -0.02$ with (a) $\beta_{10} = \beta_{20} = \omega_2 = 1$, $\omega_1 = 2$ and (b) $\beta_{10} = \beta_{20} = \omega_2 = 0.1$, $\omega_1 = -0.2$. Here the dotted (red), circle (coral) and solid (blue) lines represent nonlinearity, dispersion and diffraction parameters, respectively.

From solutions (23) and (24), the initial position and the initial phase of bright soliton pair are related to the parameters θ_{j0} and ϕ_{j0}, while that of dark soliton pair depend on the parameters X_{j0} and ψ_0. The width and the frequency shift of each soliton are decided by parameters η_j and ξ_j, which also control the separating or interacting evolutional behavior of solitons with the suitable initial separation [*cf.* Figs. 2–4]. From the expression of δ_j in solutions (23) and (24), as shown in Figs. 2 (b) and (d), the velocities of each soliton in bright and dark soliton pairs are determined by $\xi_j T$ and $(\delta + \xi_j)T$ with T satisfying Eq. (10) for chirp-free soliton and Eq. (15) for chirped one, respectively. They are both related to the parameter ξ_j and the diffraction/dispersion parameters $\beta_1(t)$ and $\beta_2(t)$. Thus, by modulating appropriate system parameters $\beta_1(t)$ and $\beta_2(t)$, we can trap the velocity of each soliton to control the interaction between soliton pairs. Meanwhile, the interaction scenarios pertaining to in-phase and off-phase injection with equal and unequal amplitudes can be dealt elaborately. The property of two separated solitons in Figs. 2 (a), 3 (a), 4 (a) and 4 (c) is significant enough to increase the bit-rate in optical communication. However, for different initial distances and velocities shown in Figs. 2 (c), 3 (b), 4 (b) and 4 (d), the interaction behaviors between soliton pairs appear, which should be avoided in the practical application.

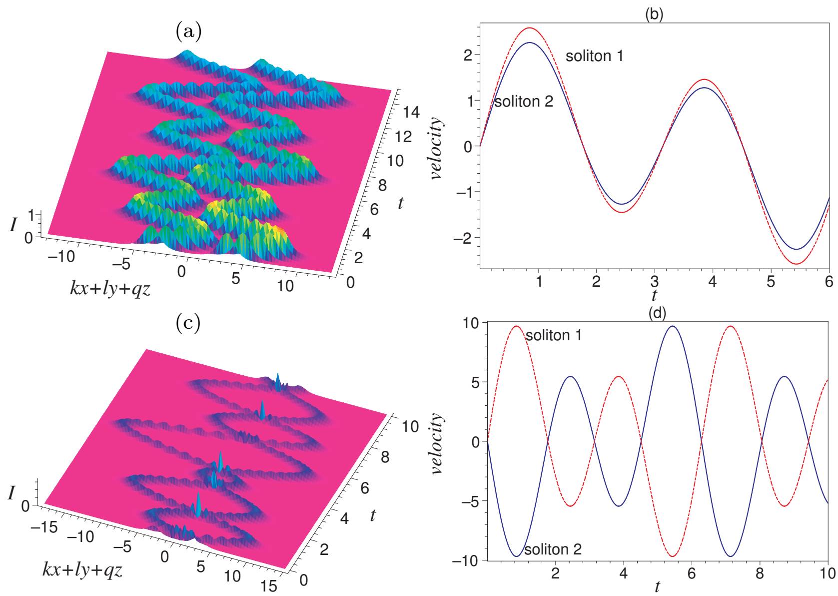

Fig. 2. (Color online) The spatiotemporal scenarios of the density distribution $I = |u|^2$ for bright soliton pair with (a) separated propagation and (c) snake-like interaction in the periodic distributed system. (b) and (d) describe the velocities of bright soliton pairs corresponding to (a) and (c). The parameters are chosen as (a) $\eta_2 = 1$, $\eta_1 = -1.1$, $\xi_1 = -\theta_{10} = 0.8$, $\theta_{20} = -\xi_2 = -0.7$, $\phi_{10} = \phi_{20} = -0.3$ and (b) $\xi_1 = -\xi_2 = 3$, $\eta_2 = \eta_1 = -1$, $\theta_{10} = -\theta_{20} = 3$, $\phi_{10} = \phi_{20} = -1$ with $p = 1$, $\phi_0 = T_0 = \omega_0 = 0$. Other parameters are the same as those in Fig. 1 (a).

As shown in Fig. 1 (a), in the periodic distributed system, the dispersion and diffraction parameters vary with the fixed amplitude and period, while the nonlinearity parameter modulates with the damped oscillating magnitude. Thus, the effect of balance between dispersion and diffraction parameters and nonlinearity parameter makes the separation distance of two separated solitons gradually decrease, displayed in Figs. 2 and 3. In contrast, in the DDF, the diffraction parameter decreases while the dispersion parameter increases with the increasing evolutional time. The nonlinearity parameter appears as transition about the time $t = 10$, namely, before $t = 10$, the value of the nonlinearity parameter varies from large to small; after $t = 10$, it changes from small to large. As a result, the interplay of the nonlinearity parameter and dispersion/diffraction parameters makes solitons transmit in a different manner. As shown in Fig. 4, before time $t = 10$, two solitons gradually separate. After time $t = 10$, two solitons approach bit by bit.

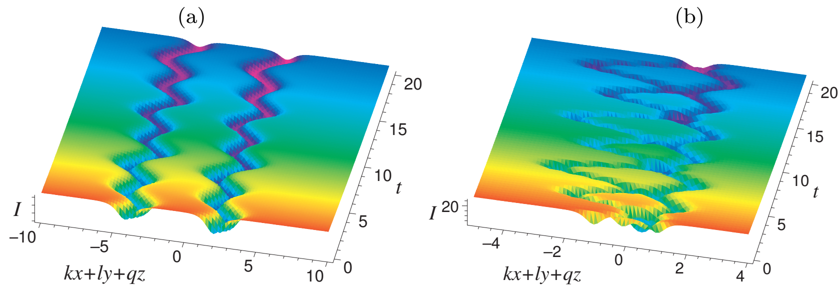

Fig. 3. (Color online) Dark soliton pair with (a) separated propagation and (b) interaction in the periodic system. The parameters are $\sigma = -\Omega = -1$, $\beta_{10} = \beta_{20} = 0.1$ with (a) $\eta_2 = \xi_1 = 1.4$, $\eta_1 = \xi_2 = 1.5$, $X_{10} = -X_{20} = 2$ and (b) $\xi_2 = -\xi_1 = 4$, $\eta_1 = \eta_2 = 3$, $X_{10} = -X_{20} = 1$. Other parameters are the same as those in Fig. 2.

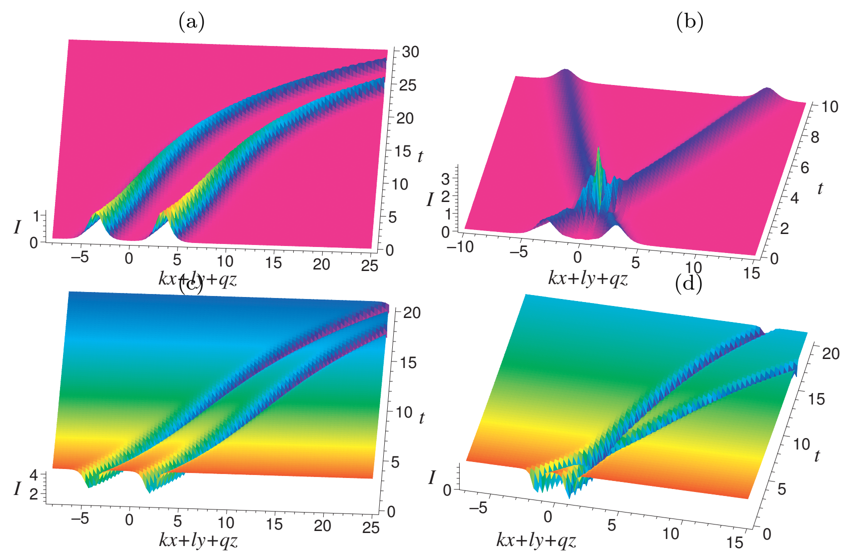

Fig. 4. (Color online) Bright and dark soliton pairs with (a), (c) separated propagation and (b), (d) interaction in the DDF. (c) and (d) describe the velocities of bright soliton pair corresponding to (a) and (b). The parameters are the same as those in Fig. 1 (b), Figs. 2 and 3 except for (a) and (b) $\beta_{10} = \beta_{20} = 0.1$ and (d) $\xi_2 = -\xi_1 = 0.6$.

5. Evolution behaviors of nonautonomous chirped soliton pairs

In this section, we will analyze the influence of the chirp on the dynamics of nonautonomous soliton pairs, which are exhibited in Figs. 5–7. From Eqs. (17) and (19), we can obtain the analytical expression of the harmonic potential in two typical nonlinear system, that is, the periodic distributed system and the DDF. For the periodic distributed system, we have $V(t) = 2c_0^2\beta_{10}\cos(\omega_1 t)r^2/\{1 - c_0\exp[2c_0\sin(\omega_1 t)/\omega_1]\}$. For the DDF, the harmonic potential has the form $V(t) = 2c_0^2\beta_{10}\exp(\omega_1 t)r^2/\{1 - c_0\exp[2c_0\exp(\omega_1 t)/\omega_1]\}$. Fig. 5 displays these harmonic potentials. We find the periodic rise or attenuation for the periodic distributed system [*cf.* Fig. 5 (a)], and the monotonous increasing for the DDF system [*cf.* Fig. 5 (c)].

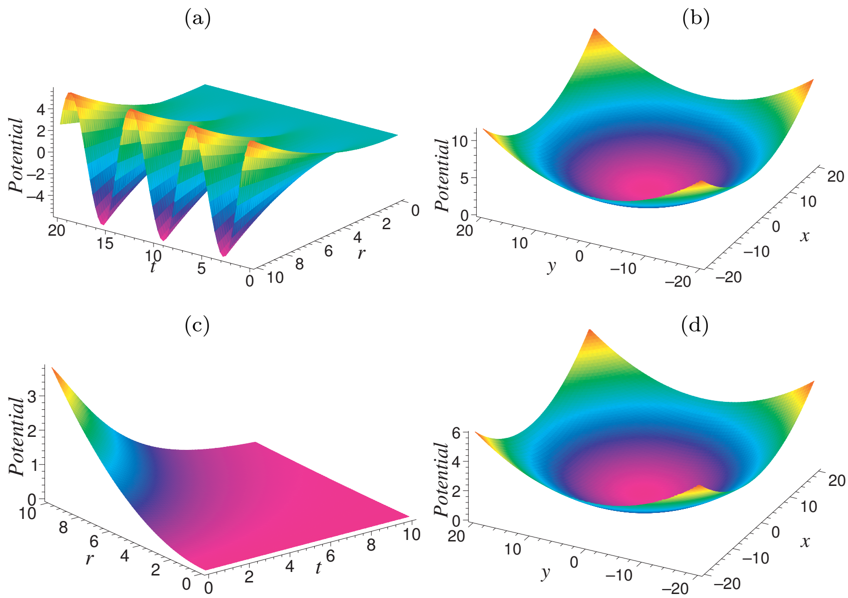

Fig. 5. (Color online) Harmonic potential in the (a), (b) periodic and (c), (d) DDF system. The parameters in (a), (b) and in (c), (d) are the same as those in Figs. 2 and 4 respectively except for $c_0 = -0.2$. (b) and (d) display the harmonic potential at time $t = 5$.

In the periodic distributed system [*cf.* Fig. 6 (a)], the dispersion/diffraction parameter changes periodically, while the nonlinearity parameter oscillates with the damped magnitude. Compared with the chirp-free bright soliton pair in Figs. 2 (a) and (c), chirped bright soliton pairs exhibit different evolutional behaviors. In Fig. 6 (c), the oscillating range of chirped bright soliton pair reduces more dramatically than that of chirp-free bright soliton pair. This variation is caused by the presence of the chirp. More

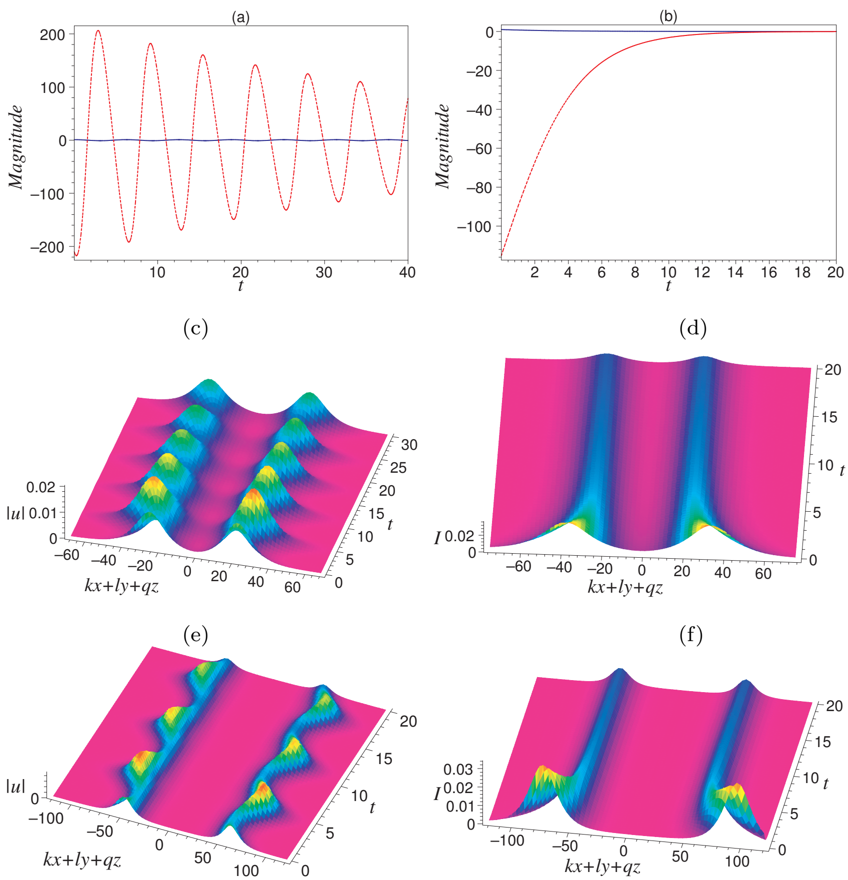

Fig. 6. (Color online) Chirped bright soliton pair in the (a), (c), (e) periodic and (b), (d), (f) DDF systems. The parameters in (c), (e) and in (d), (f) are the same as those in Figs. 2 and 4 respectively except for $c_0 = -0.2$. Here the dotted (red) and solid (blue) lines represent nonlinearity and diffraction/dispersion parameters, respectively.

specially, the chirp restrains the interaction between chirped bright soliton pair. In Fig. 2 (c), by choosing parameters η_j and ξ_j, interaction between chirp-free bright soliton pair appears. However, for the same parameters in Fig. 2 (c), the expectant interaction between chirped bright soliton pair does not happen. On the contrary, the separated propagating behavior occurs, as shown in Fig. 6 (e). Moreover, the separation between two separated propagating chirped bright soliton is bigger than that in Fig. 6 (c).

In the DDF [*c.f.* Fig. 6 (b)], the dispersion/diffraction parameter decreases by degrees, which is the same as that in Fig. 1 (b). However, the role of adding the chirp influences the nonlinear parameter. Different from

Fig. 1 (b), the transition of the changing nonlinear parameter disappears, and replacing it, the nonlinear parameter adds monotonically and reaches a maximum, which is named after the saturation nonlinearity (*i.e.* when the nonlinearity adds to this value, it will not change with the increasing evolutional time t). Thus, as seen from Fig. 6 (d) and (f), the separation between chirped bright soliton pair gradually reduces and finally inclines to a certain value when the nonlinear parameter reaches saturation nonlinearity. Similarly to the case in periodic distributed system, for the same parameters in Fig. 4 (b), the conjectural interaction between chirped bright soliton pair also does not exist, and the separated propagating behavior with the bigger separation appears, as shown in Fig. 6 (f).

Finally, we discuss the evolutional behaviors between chirped dark soliton pair in the periodic and DDF systems. In the periodic distributed system, the oscillations of $\beta_1(t)$, $\beta_2(t)$ and χ combine, as shown in Figs. 7 (a) and (b), where we also see the role of adding chirp. The chirp warps the amplitude of the signal in surprising ways. In the DDF, the chirp adds the varying magnitude of dark soliton pair. The separation between dark soliton pair gradually reduces and ultimately tends to a certain value when the saturation nonlinearity exists.

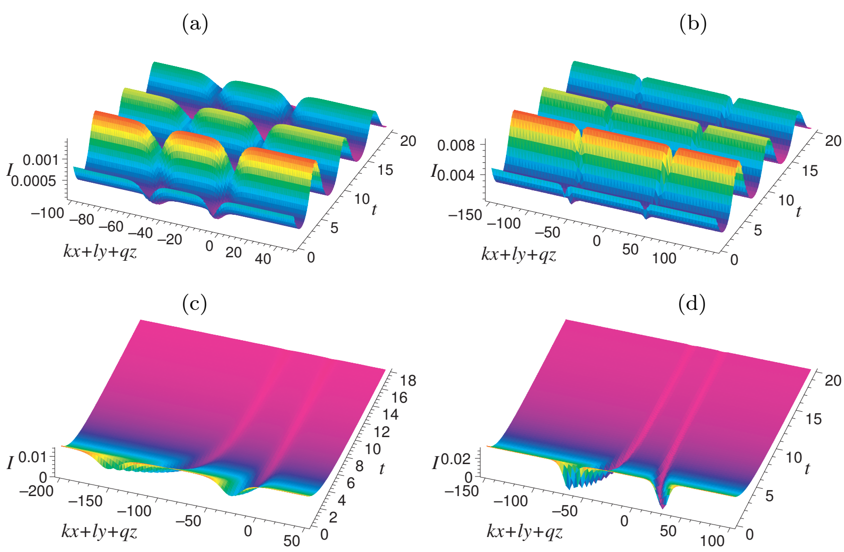

Fig. 7. (Color online) Chirped dark soliton pair in the (a), (b) periodic and (c), (d) DDF systems. The parameters (a), (b) and in (c), (d) are the same as those in Figs. 3 and 4, respectively except for $c_0 = -0.2$.

6. Conclusions

In summary, via the similarity transformation method, we present nonautonomous chirp-free and chirped solitons described by the (3+1)-dimensional generalized NLSE with variable coefficients in the presence of gain (loss) and a harmonic potential. The explicit functions, which describe the evolution of the amplitude, phase and velocity, are obtained. The gain parameter has no effect on the motion of the solitons' phases or their velocities, and it affects just the evolution of their peaks. Their dynamical behaviors in the periodic distributed and DDF systems are discussed. By modulating appropriate diffraction/dispersion parameters, we can trap the velocity of each soliton to control the interaction between soliton pairs. Parameters η_j and ξ_j control the separating or interacting evolutional behavior of chirp-free solitons with the suitable initial separation. However, the appearance of the chirp restrains the interaction between chirped soliton pairs. This property is significant to increase the bit-rate in optical communication. We expect that these results for nonautonomous solitons would have potential applications in the optical communications, long-haul telecommunication networks and BECs.

This work was supported by the National Natural Science Foundation of China (Grant No. 11005092), the Program for Innovative Research Team of Young Teachers in Zhejiang A&F University (Grant No. 2009RC01) and the Scientific Research and Developed Fund of Zhejiang A&F University (Grant No. 2009FK42).

REFERENCES

[1] R.Y. Hao, R.C. Yang, L. Li, G.S. Zhou, *Opt. Commun.* **281**, 1256 (2008); H.Y. Wu, J.X. Fei, C.L. Zheng, *Commun. Theor. Phys.* **54**, 55 (2010).

[2] C.Q. Dai, Y.Y. Wang, J.L. Chen, *Opt. Commun.* **284**, 3440 (2011).

[3] V.N. Serkin, A. Hasegawa, *Phys. Rev. Lett.* **85**, 4502 (2000); V.A. Brazhnyi, V.M. Pérez-García, *Chaos, Solitons Fractals* **44**, 381 (2011).

[4] V.N. Serkin, A. Hasegawa, T.L. Belyaeva, *Phys. Rev. Lett.* **98**, 074102 (2007).

[5] X.J. Lai, X.O. Cai, *Z. Naturforsch.* **A66**, 392 (2011).

[6] V.N. Serkin, A. Hasegawa, T.L. Belyaeva, *J. Mod. Opt.* **57**, 1456 (2010).

[7] T.L. Belyaeva *et al.*, *Laser Phys.* **21**, 1 (2011).

[8] Z.B. Cai *et al.*, *J. Math. Phys.* **52**, 053519 (2011).

[9] S.L. Xu, J.C. Liang, L. Yi, *Commun. Theor. Phys.* **53**, 159 (2010); W.P. Zhong, M. Belić, *Phys. Rev.* **E82**, 047601 (2010).

[10] J. Belmonte-Beitia, V.V. Konotop, V.M. Pérez-García, V.E. Vekslerchik, *Chaos, Solitons Fractals* **41**, 1158 (2009).

[11] Y.Z. Xia, W.P. Zhong, M. Belić, *Acta Phys. Pol. B* **42**, 1881 (2011).

[12] C.Q. Dai, Y.Y. Wang, J.F. Zhang, *Opt. Lett.* **35**, 1437 (2010); C.Q. Dai, X.G. Wang, J.F. Zhang, *Ann. Phys. (NY)* **326**, 645 (2011).

[13] J.C. Liang, H.P. Liu, F. Liu, L. Yi, *J. Phys. A: Math. Theor.* **42**, 335204 (2009).

[14] N.Z. Petrović, M. Belić, W.P. Zhong, *Phys. Rev.* **E81**, 016610 (2010).

[15] N.Z. Petrović, W.P. Zhong, *Phys. Rev.* **E81**, 056604 (2010); N.Z. Petrović, M. Belić, W.P. Zhong, *Phys. Rev.* **E83**, 026604 (2011).

[16] C.Q. Dai, Y.J. Xu, R.P. Chen, S.Q. Zhu, *Eur. Phys. J.* **D59**, 457 (2010).

[17] W.P. Zhong *et al.*, *Phys. Rev.* **A78**, 023821 (2008).

[18] C.Q. Dai, J.F. Zhang, *J. Phys. A* **39**, 723 (2006).

[19] X.J. Lai, *Commun. Theor. Phys.* **55**, 555 (2011).